CHIN. PHYS. LETT. Vol. 36, No. 3 (2019) 034203

Zero Refractive Index Properties of Two-Dimensional Photonic Crystals with Dirac Cones *

Guo-Guo Wei(魏果果), Chong Miao(苗宠), Hao-Chong Huang(黄昊翀), Hua Gao(高华)**
School of Science, China University of Geosciences, Beijing 100083

(Received 19 November 2018)

The zero refractive index properties of two-dimensional photonic crystals (PCs) are studied theoretically. Three necessary conditions for PCs to mimic the zero index materials (ZIMs) are obtained. In addition, through a comparative study of the properties for two representative PC structures with different types of Dirac cones, we find that the PC with a Dirac-like cone which meets the three necessary conditions does not behave as a ZIM in some cases. Further analysis shows that its non-zero index properties originate from the flat dispersion band. These findings clarify the fundamental physical issue of which type of Dirac cone PC can mimic a real ZIM.

PACS: 42.25.Bs, 42.70.Qs, 41.20.Jb DOI: 10.1088/0256-307X/36/3/034203

In recent years, zero index materials (ZIMs) have attracted great interest for their powerful manipulation of electromagnetic waves. All kinds of peculiar optical effects have been achieved via ZIMs, which include total reflection or total transmission,[1] directional emission,[2] tunneling waveguides,[3] electromagnetic cloaks,[4] electromagnetic shielding,[5] laser ignition,[6] optical unidirectional transmission (UDT),[7] and so on. In addition, some novel kinds of ZIMs were also proposed to implement some unique functions; for example, anisotropic ZIMs can realize the spatial power combination for omnidirectional radiation.[8,9] Magnetic ZIMs can implement ZIM functions at a flexible operating frequency.[10,11] Doped semiconductors can exhibit a near-zero permittivity with the additional advantages of being a CMOS-compatible platform.[12] Topological insulators can exhibit an epsilon-near-zero response at ultraviolet frequencies.[13]

Recently, a class of photonic crystals (PCs) with conical dispersion at $K = 0$ has been demonstrated to have zero refractive index (ZRI) near the Dirac point.[14–16] This kind of PC ZIM has attracted much attention since they were proposed because of their non-absorption, matched impedance to the free space and freely tunable frequency.[17–24] This novel PC ZIM indicates that the conical dispersions and the ZRI must be related in a certain way. Thus, it is interesting to study the relationship between them. Moreover, the Dirac cones in PCs can be classified into three different types (Dirac cone, Dirac-like cone and double Dirac cone). Do the three types of Dirac cone play the same role in realizing a ZIM? To answer these questions, we first theoretically study the relationship between the conical dispersions and the ZRI, and three necessary conditions for PCs to mimic ZIMs are obtained. In addition, we comparatively study the propagation and transmission properties of the PCs with two different types of Dirac cone possibly located at the Γ point. The role of the non-conical dispersion band is investigated carefully. All the findings clarify the basic physical issue of which type of Dirac cone PC can mimic a real ZIM.

We select a two-dimensional (2D) system to analyze our issue. In a 2D PC with a Dirac cone, the light wave with electric component polarized in the z direction meets the 2D massless Dirac equation[25]

$$\begin{pmatrix} 0 & -iV_{\rm D}\left(\frac{\partial}{\partial x} - i\frac{\partial}{\partial y}\right) \\ -iV_{\rm D}\left(\frac{\partial}{\partial x} + i\frac{\partial}{\partial y}\right) & 0 \end{pmatrix} \begin{pmatrix} \psi_1 \\ \psi_2 \end{pmatrix} = (\omega - \omega_{\rm D}) \begin{pmatrix} \psi_1 \\ \psi_2 \end{pmatrix}, \tag{1}$$

where ψ_1 and ψ_2 are the two eigenfunctions of the electric fields with the same frequency ω, $V_{\rm D}$ is the group velocity, and $\omega_{\rm D}$ is the frequency of the Dirac point. Inside the PC, the light wave should also meet the Maxwell equations. If the PC can be regarded as a homogenous material, the Maxwell equations are reduced to the Helmholtz equation

$$\left(\frac{\partial^2}{\partial x^2} + \frac{\partial^2}{\partial y^2}\right)\psi + k^2\psi = 0, \tag{2}$$

where the acting operator can be expanded as

$$\frac{\partial^2}{\partial x^2} + \frac{\partial^2}{\partial y^2} = \begin{pmatrix} 0 & \frac{\partial}{\partial x} - i\frac{\partial}{\partial y} \\ \frac{\partial}{\partial x} + i\frac{\partial}{\partial y} & 0 \end{pmatrix} \cdot \begin{pmatrix} 0 & \frac{\partial}{\partial x} - i\frac{\partial}{\partial y} \\ \frac{\partial}{\partial x} + i\frac{\partial}{\partial y} & 0 \end{pmatrix}. \tag{3}$$

We make this substitution in Eq. (2), and write ψ in the matrix of $\begin{pmatrix} \psi_1 \\ \psi_2 \end{pmatrix}$, and obtain

$$\begin{pmatrix} 0 & -i(\frac{\partial}{\partial x} - i\frac{\partial}{\partial y}) \\ -i(\frac{\partial}{\partial x} + i\frac{\partial}{\partial y}) & 0 \end{pmatrix} \cdot \begin{pmatrix} 0 & -i(\frac{\partial}{\partial x} - i\frac{\partial}{\partial y}) \\ -i(\frac{\partial}{\partial x} + i\frac{\partial}{\partial y}) & 0 \end{pmatrix} \begin{pmatrix} \psi_1 \\ \psi_2 \end{pmatrix} = k^2 \begin{pmatrix} \psi_1 \\ \psi_2 \end{pmatrix}. \tag{4}$$

*Supported by the National Natural Science Foundation of China under Grant Nos 11504336 and 61805214, and the Fundamental Research Funds for the Central Universities under Grant No 265201430.
**Corresponding author. Email: gaohua@cugb.edu.cn

By applying Eq. (1) two times in Eq. (4), we obtain

$$k^2 = \left(\frac{\omega - \omega_{\rm D}}{V_{\rm D}}\right)^2. \quad (5)$$

At the Dirac point

$$k^2_{\omega=\omega_{\rm D}} = (k_{xr} + ik_{xi})^2 + (k_{yr} + ik_{yi})^2 = 0, \quad (6)$$

where k_{xr}, k_{xi}, k_{yr} and k_{yi} are the real and imaginary parts of the wave vector in the x and y directions, respectively. If the Dirac point is located at the Γ point ($k_{xr} = 0$, $k_{yr} = 0$), the imaginary parts will also be zero. Therefore, the effective refractive index of this kind of PC is zero. In such a case, the PC can behave as a ZIM. In contrast, if the Dirac cone is not located at the Γ point, none of the real parts and the imaginary parts of the wave vector will be zero, and correspondingly the PC will have a nonzero effective refractive index. The above analysis means that to mimic a ZIM, the PC must meet three conditions: firstly, the dispersion relations near the Dirac point are conical. Secondly, the Dirac point is located at the Γ point. Thirdly, the PC can be regarded as a homogenous material. The last condition is indispensable, while it is frequently neglected. For example, at some high frequencies, even the conical dispersions are formed at the Γ point, and the PCs still do not possess zero index properties.[19] The reason is that they cannot be regarded as homogenous materials and Eq. (2) cannot be used.

From the above analysis, it is known that the ZRI of the PCs is only attributed to the conical dispersion. And then, what is the effect of the non-conical dispersion band near the Dirac cone? To answer this question, we select a double Dirac cone which consists of two pairs of Dirac cones overlapping at the Dirac point and a Dirac-like cone which consists of a Dirac cone and a flat band also intersecting at the Dirac point to compare them and identify the effect of the flat band. For the Dirac-like cone PC (DL-PC), we choose a PC consisting of dielectric rods with a square lattice as illustrated in the inset of Fig. 1(a). Its band diagram for transverse electric (TE) polarization (the electric field is along the z-axis) is calculated using a commercial software FDTD solutions. In the calculation, the radius and the permittivity of the dielectric rods are set to be $R = 0.2a$ and $\varepsilon = 12.5$, respectively, where a is the lattice constant. The calculated band structure is shown in Fig. 1(a), which shows that two linear dispersion lines insect at the Γ point with the Dirac point frequency of $0.541\omega a/2\pi c$. Moreover, there is an additional flat band crossing the two conical bands at the Γ point, resulting in a threefold degeneration, forming a Dirac-like cone. For the double Dirac cone PC (DD-PC), we choose a PC with a triangle lattice consisting of dielectric cylindrical shells as illustrated in the center of Fig. 1(b). The outer and inner radii of the dielectric shells are $R = 0.45a$ and $r = 0.2656a$, respectively, and the permittivity of the shells is $\varepsilon = 12$. We also consider the case of TE polarization and the calculated band structure is shown in Fig. 1(b). It is seen that four bands linearly intersect at a four-fold degenerate point, forming two pairs of cones located at the Γ point and at a frequency of $0.404\omega a/2\pi c$. Unlike the Dirac-like cone, in addition to the four conical dispersion bands, there is no other non-conical band near the double Dirac point. In the following calculation and analysis, the lattice constants for the two PCs both take the value of $a = 0.5\,\mu$m. Accordingly, the wavelengths at the Dirac points of the two PCs are $0.9227\,\mu$m and $1.2387\,\mu$m, respectively.

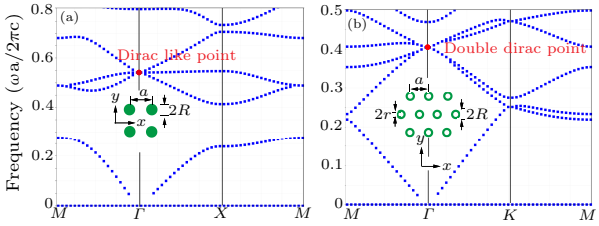

Fig. 1. Photonic band structures for two different 2D dielectric PCs. The inset in each band structure depicts its PC structure and the coordinate system.

We put an electric dipole source inside the two PCs and set its frequency to be exactly the Dirac point frequency for each PC. Furthermore, to be consistent with the polarization state of the band structure, the electric field of the dipole source also takes the direction along the z-axis. The waves emitted from the dipole resource and scattered by the rods (cylindrical shells) can be regarded as propagating in all directions. Thus all the permitted propagation modes, not only the conical dispersion bands but also the non-conical dispersion band, are excited in the PCs. Then we observe their propagation properties inside and outside the two PCs.

Figure 2 gives the stabilized electric field distributions when the electric dipole is put inside a slab made up of the PCs with a corner cut away, where the white circles indicate the positions of the dipole sources. Figures 2(a) and 2(b) represent the DL-PC and the DD-PC, respectively. From the field distributions shown in Fig. 2, it is seen that there is a distinct difference between the two fields. For the DL-PC, both inside and outside the slab, the propagating directions of the light are chaotic. Though the exit surfaces are planes, their wave fronts are not parallel to the exit surfaces and are even hard to identify. This means that the wave front shaping function of the ZIM does not work here. In contrast, for the DD-PC, no matter which direction the exit surfaces are along, the outgoing directions of the propagating waves are always perpendicular to the exit surfaces. According to the Snell law, it can be deduced that the effective refractive index of the DD-PC is zero. Secondly, because of the influence of the dipole, the fields in both the PCs are non-uniform. However, the field in the DD-PC tends to become uniform as it goes further away from the dipole source while the field in the DL-PC does not manifest such a tendency. It is known that if the PC has an effective zero index, the field should become more and more uniform, thus we can infer from the field distributions that the DL-PC does not have an effective ZRI.

Another fascinating property of the ZIMs is that light is totally reflected at large incident angles while it is transmitted under normal incidence. This effect is a direct consequence of the Snell law when it is applied to ZIMs. Figure 3 gives the transmittance through a parallel slab made up of the two different PCs as a function of the incident angle. The blue dashed line and the red solid line represent the transmission curves for the DD-PC and the DL-PC, respectively. In the calculation, the layer numbers of the two PCs are both taken to be 26. It is worth mentioning that, to obtain the matched impedance to free space for the DD-PC, we truncate the first and last layers of the cylindrical shells with a cutting parameter of $L = 1.866R$, as carried out in Ref. [24]. The same operations are also performed in Figs. 4(b) and 5(c). Obviously, if the incident angle is small enough, the maximum transmittance of unit 1 is obtained for both the PCs. However, with the increase of the incident angle, the transmittance of the DD-PC decreases rapidly to zero in 5°, which agrees well with the property of an ideal ZIM. However for the DL-PC, its transmittance does not decrease monotonically. At several incident angles, the transmittances even increase dramatically and several resonant transmission peaks up to 1 appear. Their electric intensity patterns at the resonant angles are extracted and given in the insets in Fig. 3. By investigating the properties of these resonances, we find that they are Fabry–Perot resonances between the two interfaces of the slab. Because the phase change of a round trip inside a ZIM slab is zero, these resonances further prove that the effective refractive index of the DL-PC is not zero.

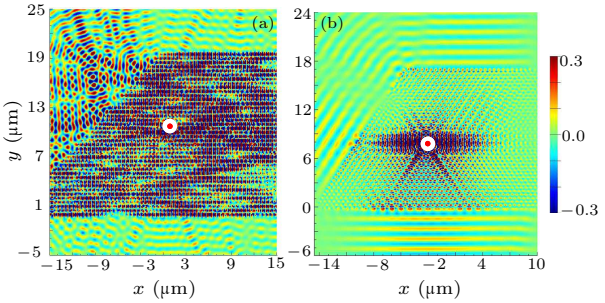

Fig. 2. The stabilized electric field distributions when a dipole source is placed inside a DL-PC slab (a) and a DD-PC slab (b) with a corner cut away, where the white circles indicate the locations of the dipole sources.

From the above investigation, we know that when the flat band is excited, the DL-PC does not present zero index properties. Here we would like to ask the question why the zero index properties as well as their applications are still obtained although the flat band always exists in the PCs.[14] Through careful study, we find that all the incident directions upon the DL-PC are normal incidence and this particular incident condition avoids the excitation of the flat band mode with a nonzero tangential wave vector. For normal incidence, the tangential component of the wave vector is $k_x = 0$, and according to the conservation of the wave vector along the interface, the tangential wave vector inside the PC should also hold zero. Therefore, the modes with a nonzero k_x component of the flat band cannot be excited and the PC still presents zero index properties. Examples of zero index applications, such as wave front shaping, cloaking and focusing are all obtained.[14] As an example, Fig. 4 gives the distributions of the electric field when a plane wave is incident normally upon the PC slab used in Fig. 2. The blue arrows represent the incident directions and the red arrows depict the outgoing directions. It is seen that under this incident condition, inside the two PCs, only the zero index mode can be excited, thus the field is almost uniform throughout the whole PC. Furthermore, the propagation directions outside the PCs are all perpendicular to the exit surfaces. Obviously, under normal incidence, at Dirac frequency, when the flat band mode with the nonzero tangential wave vector of the DL-PC is suppressed, this PC still behaves as a ZIM, while for the DD-PC, it always presents zero index property no matter what incident condition is taken.

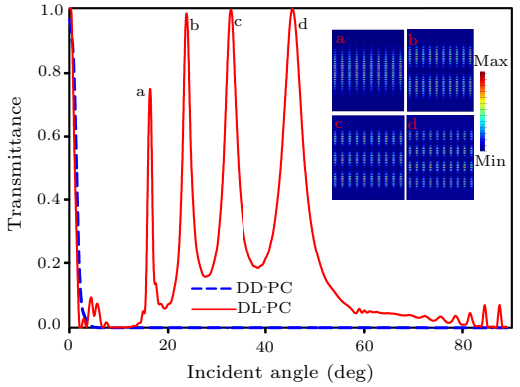

Fig. 3. Transmittances as a function of the incident angle for two PC slabs, where the red solid curve represents the DL-PC and the blue dashed curve represents the DD-PC. The insets in the top right corner are the electric intensity distributions inside the DL-PC slab at the corresponding resonant incident angles.

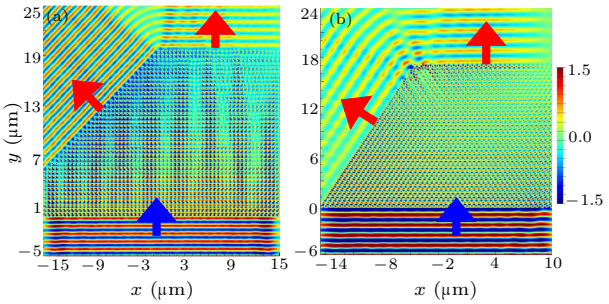

Fig. 4. The outgoing directions of the light wave from a DL-PC slab (a) and a DD-PC slab (b) with a corner cut away when a plane wave at each Dirac point frequency is incident normally from the bottom.

To further demonstrate the differences of the two PCs in implementing the functions of the ZIM, we design a UDT structure based on the transmission property of the ZIM. It is a dielectric grating and a ZIM slab cascaded structure, as shown in Fig. 5(a). By tuning the thickness of the dielectric grating, the efficiency of the zeroth diffraction order can be adjusted to zero and all of the intensity is concentrated

to the higher orders.[26] When light is incident from the ZIM side normally, it will firstly transmit through the ZIM and then be diffracted by the dielectric grating to the other side. In contrast, if the light is incident from the grating side, it will be diffracted to higher orders and then all these diffracted beams are obliquely incident on the ZIM slab and reflected by the ZIM slab. Thus, different transmittances will be obtained when the light is incident upon this cascaded structure from the opposite directions, and the UDT effect is achieved. Here we use the two kinds of PCs as the ZIM individually. If the PC has zero index, the UDT effect will be obtained. In contrast, if the PC is not a ZIM, this one-way transmission effect will not be achieved. Figures 5(b) and 5(c) give the electric field distributions for the opposite incidences. In calculation, we set the period and the filling factor of the grating to be $p = 3\,\mu\text{m}$ and $w/p = 0.5$, respectively. The refractive index of the grating dielectric is taken to be $n = 1.4$. In the field distributions, the black arrows represent the incident directions and the pink rectangles represent the positions of the dielectric grating strips. To ensure the efficiencies of the zeroth order diffraction in the two structures are both zero, the thicknesses of the grating strips are selected to be different as $H = 1.32\,\mu\text{m}$ and $H = 1.62\,\mu\text{m}$.

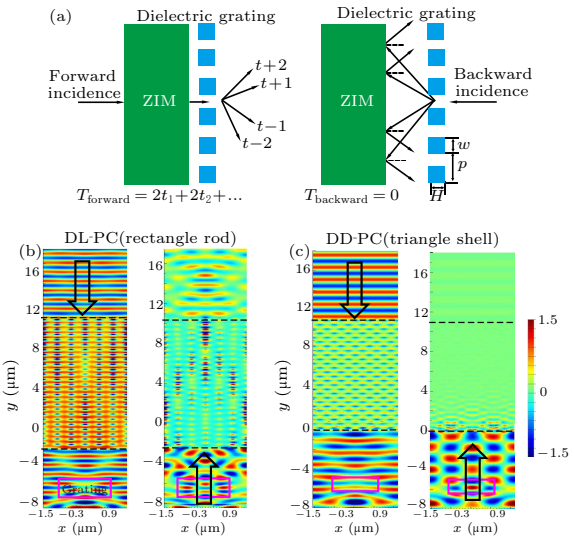

Fig. 5. (a) The unidirectional transmission mechanism of a ZIM slab and a dielectric grating cascaded structure. (b), (c) The electric field distributions for opposite incident directions using the two kinds of PC as the ZIM, respectively.

From the distribution of the two fields, it is seen that the UDT effect is only obtained using the DD-PC as a ZIM. The fields inside the DD-PC are nearly uniform for both the forward and backward incident directions which agree well with the ZIM. As for the DL-PC structure, when light is incident from the grating side, its transmission is not completely restrained. In addition, the fields inside the DL-PC are inhomogeneous for both incident directions, which further demonstrates that the DL-PC does not behave as a ZIM.

In conclusion, we have theoretically studied the relationship between the Dirac cone dispersion and the ZRI. We also study the flat band effect of the Dirac-like cone on realizing the ZIM. All the findings show that, to mimic ZIMs, the PCs must satisfy the following conditions: Firstly, there exist only conical dispersion relations near the Dirac point. Secondly, the Dirac point must be located at the center of the first Brillouin zone. Thirdly, the PC can be regarded as a homogenous material for light waves propagating inside it.

References

[1] Nguyen V C, Chen L and Halterman K 2010 *Phys. Rev. Lett.* **105** 233908
[2] Enoch S, Tayeb G, Sabouroux P, Guerin N and Vincent P 2002 *Phys. Rev. Lett.* **89** 213902
[3] Silveirinha M and Engheta N 2006 *Phys. Rev. Lett.* **97** 157403
[4] Hao J M, Yan W and Qiu M 2010 *Appl. Phys. Lett.* **96** 101109
[5] Zhai T R, Shi J W, Chen S J and Liu D H 2011 *Appl. Phys. Express* **4** 074301
[6] Zhai T R, Shi J W, Chen S J, Liu D H and Zhang X D 2011 *Opt. Lett.* **36** 2689
[7] Fu Y, Xu L, Hang Z H and Chen H 2014 *Appl. Phys. Lett.* **104** 193509
[8] Zhu W R, Rukhlenko I D and Premaratne M 2012 *Phys. Rev. Lett.* **108** 213903
[9] Wang N, Chen H J, Lu W L, Liu S Y and Lin Z F 2013 *Opt. Express* **21** 23712
[10] Yu X N, Chen H J, Lin H X, Zhou J L, Yu J J, Qian C X and Liu S Y 2014 *Opt. Lett.* **39** 4643
[11] Lin H X, Yu X N and Liu S Y 2015 *Acta Phys. Sin.* **64** 034203
[12] Kinsey N, Devault C, Kim J, Ferrera M, Shalaev V M and Boltasseva A 2015 *Optica* **2** 616
[13] Ou J Y, So J K, Adamo G, Sulaev A and Wang L 2014 *Nat. Commun.* **5** 5139
[14] Huang X, Lai Y, Hang Z H, Zheng H and Chan C T 2011 *Nat. Mater.* **10** 582
[15] Moitra P, Yang Y, Anderson Z, Kravchenko I I, Briggs D P and Valentine J 2013 *Nat. Photon.* **7** 791
[16] Li Y, Kita S, Muñoz P, Reshef O and Vulis D I 2015 *Nat. Photon.* **9** 738
[17] Mei J, Wu Y, Chan C T and Zhang Z Q 2012 *Phys. Rev. B* **86** 035141
[18] Chen Z G, Ni X, Wu Y, He C, Sun X C, Zheng L Y, Lu M H and Chen Y F 2015 *Sci. Rep.* **4** 4613
[19] Ashraf M W and Faryad M 2016 *J. Opt. Soc. Am. B* **33** 1008
[20] Fang K, Zhang Y, Li F, Jiang H and Li Y 2012 *Opt. Lett.* **37** 4654
[21] Dong J W, Chang M L, Huang X Q, Hang Z H, Zhong Z C, Chen W J, Huang Z Y and Chan C T 2015 *Phys. Rev. Lett.* **114** 163901
[22] Boriskina S V 2015 *Nat. Photon.* **9** 422
[23] D'Aguanno G, Mattiucci N, Conti C and Bloemer M J 2013 *Phys. Rev. B* **87** 085135
[24] Li Y and Mei J 2015 *Opt. Express* **23** 12089
[25] Sepkhanov R A, Bazaliy Y B and Beenakker C W J 2007 *Phys. Rev. A* **75** 063813
[26] Gao H, Ouyang M, Wang Y, Shen Y, Zhou J and Liu D H 2007 *Optik* **118** 452